31st Annual International Conference of the IEEE EMBS
Minneapolis, Minnesota, USA, September 2-6, 2009

Induced Respiratory System Modeling by High Frequency Chest Compression Using Lumped System Identification Method

Jongwon Lee, *Member, IEEE,* Yong Wan Lee, George O'Clock, *Life Member, IEEE,* Xiaoming Zhu, Keshab K. Parhi, *Fellow ,IEEE,* Warren J. Warwick

***Abstract*—High frequency chest compression (HFCC) treatment systems are used to promote mucus transport and mitigate pulmonary system clearance problems to remove sputum from the airways in patients with Cystic Fibrosis (CF) and at risk of developing chronic obstructive pulmonary disease (COPD). Every HFCC system consists of a pump generator, one or two hoses connected to a vest, to deliver the pulsation. There are three different waveforms in use; symmetric sine, the asymmetric sine and the trapezoid waveforms. There have been few studies that compared the efficacy of a sine waveform with the HFCC pulsations. In this study we present a model of the respiratory system for a young normal subject who is one of co-authors. The input signal is the pressure applied by the vest to chest, at a frequency of 6Hz. Using the system model simulation, the effectiveness of different source waveforms is evaluated and compared by observing the waveform response associated with air flow at the mouth. Also the study demonstrated that the ideal rectangle wave produced the maximum peak air flow, and followed by the trapezoid, triangle and sine waveform. The study suggests that a pulmonary system evaluation or modeling effort for CF patient might be useful as a method to optimize frequency and waveform structure choices for HFCC therapeutic intervention.**

I. Introduction

High frequency chest compression (HFCC) is one of the effective therapeutic methods used to assist the clearance of sputum associated microorganisms from the infected respiratory systems of chronic obstructive pulmonary disease (COPD). The HFCC mechanical system consists of three major components: (1) the pulse generator source that is designed to adjust frequencies and pressures to produce pulsations, (2) the tubing that deliver the pulses to the chest and (3) a vest that covers the patient's chest and applies the oscillatory and compression pressure waveforms to the chest wall and then to the airways in the lungs. The energy reaching the pulmonary system is transported through the airway lung system and finally exits the mouth as with a certain pressure and airflow rate. The intensities and shapes of the pressure and air flow waveforms are affected by the structure of the airways and the chronic obstructive changes that have been developed by the nature of the sputum in the airways.

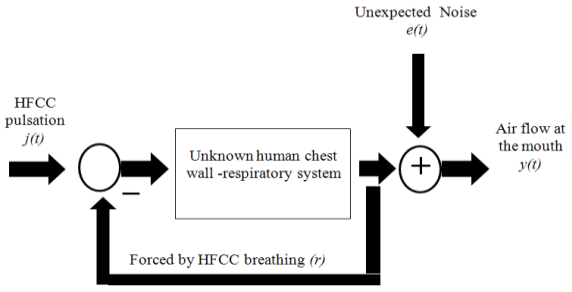

Fig. 1. (a) The modeling of HFCC and human respiratory system. In this study we used the feedback structure from the observation of respiratory signal measured from the jacket.

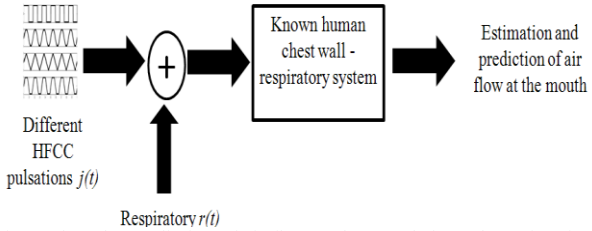

Fig. 1. (b) The prediction of air flow at the mouth from the estimation system function. Here, we simulated with 4 different HFCC pulsations at 6Hz.

A significant amount of research has been suggested to evaluate the efficacy of HFCC in terms of measuring the amount of induced air volume at the mouth, the amount of cleared dried or wet sputum, the amount of gas exchange rate of N_2, O_2 and CO_2 during the expiration and inspiration [1]-[5]. Some other additional research has shown HFCC effects on the heart rate variability, cardio-respiratory synchronization and sinus arrhythmia during HFCC therapy [6]-[7].

RC circuit, RLC circuit, extended RLC, Mead's model, DuBois, Viscoelatstic models have been introduced to estimate the resistance, compliance and inertance of normal and abnormal respiratory systems; their corresponding

Manuscript received March 23, 2009. This work was supported in part by the Defense of the lungs project sponsored by Minnesota Cystic Fibrosis Center under the guidance of Warren J. Warwick, MD..

J. Lee is with the Department of Pediatrics, University of Minnesota, Minneapolis, MN 55455 USA (corresponding author to provide phone: 612-625-2672; e-mail: jongwona@gmail.com).

Y. W. Lee is with the Department of Pediatrics, University of Minnesota, Minneapolis, MN 55455 USA (e-mail: leeyongwan@gmail.com).

George O'Clock is with the Department of Pediatrics, University of Minnesota, Minneapolis, MN 55455 USA (e-mail: george.oclock@mnsu.edu).

Xiaoming Zhu is with the Department of Electrical Engineering, University of Minnesota, Minneapolis, MN 55455 USA (e-mail: xmzhu@umn.edu).

Keshab K. Parhi is with the Department of Electrical Engineering, University of Minnesota, Minneapolis, MN 55455 USA (e-mail: parhi@umn.edu).

W. J. Warwick MD is with the Department of Pediatrics, University of Minnesota, Minneapolis, MN 55455 USA (phone: 612-624-7175; fax: 612-624-0413; e-mail: warwi001@umn.edu).

parameters were analyzed to compare normal and abnormal cases [8]-[12]. Also, the respiratory system with HFCC pulsations was analyzed with an electric circuit model for 16 air way generations for jacket pressure and air flow at the mouth from normal subjects [13]-[14]. In this study, we present the model of a respiratory system involving the chest input, which was measured at the vest and air flow at the mouth as the output during the HFCC therapy (Fig.1 (a)). We used the system identification method to develop the transfer function that relates output to input. For the next step, we simulated how the different input pressure waveforms such as sine, trapezoid, triangle and rectangle waveforms were changed at the mouth with respect to in air flow (Fig.1 (b)). Those changes can give us information how each waveform is changed through the chest wall, lung tissue and respiratory system. Finally, we analyzed and compared the efficacy of each waveform by examining its peak air flow rate.

II. METHODOLOGY

A. System Identification of HFCC-Respiratory system

System identification is a method to build a model to describe the relation between measured input and output data with estimating the transfer function. In our system model (Fig.1.), during the measurement period, input (1) and output (2) are defined from the measured data:

$$\text{Input } x(t) = r(t) + j(t) \quad (1)$$

$$r(t): Estimated\ respiratory\ signal$$

j(t) *: Pressure at the jacket*

$$\text{Output } y(t) = G(q)x(t) + H(q)e(t) \quad (2)$$

where q is the time delay factor and $G(q)x(t)$ is from the following notations[15]-[17],

$$G(q)x(t) = \sum_{k=1}^{N} g(k)x(t-k) \quad (3)$$

and

$$G(q) = \sum_{k=1}^{\infty} g(k)q^{-k} \quad (4)$$

$$q^{-k}x(t) = x(t-k) \quad (5)$$

Here, $g(k)$ and $e(t)$, respectively, represent the impulse response of the system at time k and the unexpected noise function. The function $G(q)$ is the transfer function between the input $x(t)$ and output $y(t)$. In other expression,

$$G(q) = \frac{Y(q)}{X(q)} \ (q = e^{j\omega}) \quad (6)$$

By the commonly used parametric model,

$$G(q) = q^{-nk}\frac{B(q)}{A(q)} \quad (7)$$

$$H(q) = \frac{1}{A(q)} \quad (8)$$

The model structure can be expressed in the polynomial form in the order of q^{-1}

$$A(q)y(t) = \frac{B(q)}{F(q)}x(t-nk) + \frac{C(q)}{D(q)}e(t) \quad (9)$$

$$A(q) = 1 + a_1q^{-1} + a_2q^{-2} + \ldots\ldots + a_{na}\,q^{-na} \quad (10)$$

$$B(q) = b_1 + b_2q^{-1} + b_3q^{-2} + \ldots\ldots + b_{nb}\,q^{-nb+1} \quad (11)$$

$$C(q) = c_1 + c_2q^{-1} + c_3q^{-2} + \ldots\ldots + c_{nc}\,q^{-nc+1} \quad (12)$$

$$D(q) = 1 + d_1q^{-1} + d_2q^{-2} + \ldots\ldots + \mathrm{d}_{nd}\,q^{-nd} \quad (13)$$

$$F(q) = 1 + f_1q^{-1} + f_2q^{-2} + \ldots\ldots + \mathrm{f}_{nd}\,q^{-nf} \quad (14)$$

In this study, we assumed $nc = nd = nf = 0$ (ARX structure model) and our model between the input and output can be explicitly expressed as follows:

When we define *nk* is the number of delays from the input to output, the model between the input and output can be expressed as follows:

$$A(q)y(t) = B(q)x(t-nk) + e(t) \quad (15)$$

or

$$y(t) + a_1y(t-1) + \ldots\ldots + a_{na}\,y(t-na) = b_1x(t-nk) + b_2x(t-nk-1)\ldots\ldots + b_{nb}\,x(t-nk-nb+1) + e(t) \quad (16)$$

To estimate the parameters, first we define error function *e(t)* from the Equation (16):

$$e(t) = A(q)y(t) - B(q)x(t-nk) \quad (17)$$

To determine G and H, we use the least predication error method.

$$J[A(q), B(q)] = argmin \sum_{t=1}^{N} e^2(t)$$

$$= argmin \sum_{t=1}^{N} [A(q)y(t) - B(q)x(t-nk)]^2(t) \quad (18)$$

From the equation (16), we define

$$\theta = [\,\theta_1\ \theta_2\ \theta_3\ \ldots\ldots\theta_{na+nb}\,]^T \quad (19)$$

$$\varphi_y(k) = [y(k-1)\ y(k-2)\ldots y(k-na)] \quad (20)$$

$$\varphi_x(k) = [x(k-1)\ x(k-2)\ldots y(k-nb)] \quad (21)$$

$$\varphi(k) = \left[\varphi_y(k)\ \varphi_x(k)\right] \quad (22)$$

The model can be expressed in matrix formation

$$Y = \emptyset \cdot \theta \quad (23)$$

Finally, the estimated parameters can be obtained from the equation (24)

$$\hat{\theta} = (\emptyset^T \cdot \emptyset)^{-1} \cdot \emptyset^T \cdot Y \quad (24)$$

B. Data acquisition

We measured air flow rate at the mouth *y(t)* and pressure at the jacket *x(t)* simultaneously in units of voltage during the ICS HFCC therapy (Respiratory Technologies, Inc., St. Paul, MN) from one of our co-authors, YW Lee, whose peak air flow at the mouth was 2.8 l/s. This system was recently developed and has 10 pressure settings of from 10 to 100% of maximum pressure with a frequency range of 5-30 Hz. In this study, we selected 6Hz and 100% of maximum pressure setting with a pressure range of 6-31 mmHg and an 18.5 mmHg mean pressure value. To measure flow rate at the mouth, we used the Model 3800 Hans Rudolf pneumotachometer of with differential pressure transducer (860 Series by Auto Tran, MN). At the same time, we used a Honeywell 40PC001B1A bi-directional pressure transducer and measured the pressure from the interior of back. The data from the sensors were connected to the data acquisition board

(NI-DAQ 6024 E) with sampling rate of 1000 samples/sec and output range of ± 10 Volts.

III. RESULTS

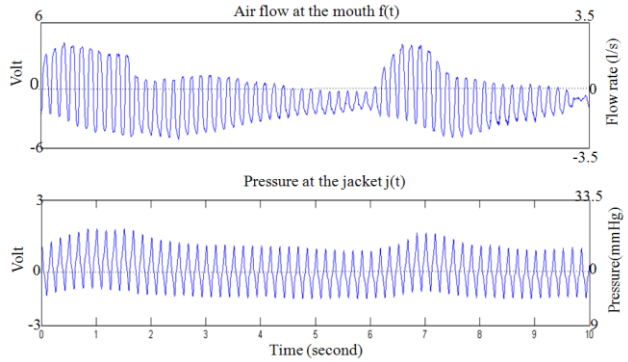

Fig. 2.The air flow at the mouth and pressure at the jacket for 10 seconds of total 300 seconds measurement time from the subject. Here positive values represent of inspiration, and negative values represent of expiration.

Air flow at the mouth and pressure at the jacket were measured for 300 seconds from the subject. We used a 5Hz low-pass filter to separate the respiratory signal *r(t)* from the air flow at the mouth *f(t)*. Their results, over a 10 second time interval (two breathing cycles) are shown in Fig. 2. The respiratory signal that is superimposed on the HFCC pulsation is influenced by chest wall or muscle movement during respiration.

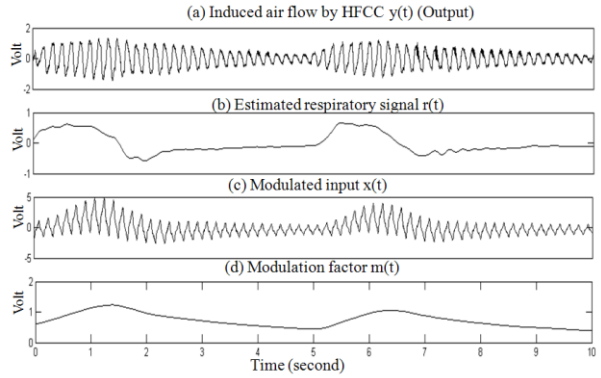

Fig. 3(a)-(d). Assigning input and output from the measured data. Output (a) represents the high-pass filtered signal from the air flow at the mouth. Estimated respiratory signal (b) was obtained from the low-pass filter output. (c) and (d) represent the input *x(t)* and modulation factor *m(t)*.

The induced air flow *y(t)* by HFCC was isolated using high-pass filtering (designated as output in Fig.3.(a)). It represented the estimated breathing activity of inspiration (positive values) and expiration (negative values) obtained from the low-pass filter (Fig.3. (b)). The phase delay between pressure at the jacket and air flow at the mouth was determined from the maximum inspiration points that pressure at the jacket *j(t)*. The phase delay is lagging at 0.38 second per breathing cycle. We added the jacket pressure *j(t)* to *r(t)* which was obtained from low-pass filter to estimate the system. The final input signal of Fig 3.(c)(with a modulation

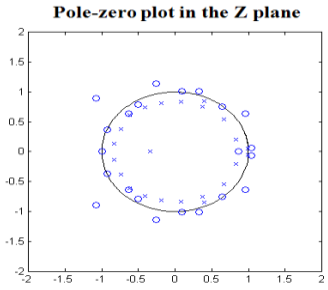

Fig. 4.Poles and zeros of the chest wall-lung respiratory system in the z-plane. In this simulation we obtained 23 poles and zeros are associated with for transfer function between input and output.

factor representing the effects of pulmonary system nonlinearities) is shown in Equation (25).

$$Input\ x(t) = \{j(t) + r(t)\} \cdot m(t) \quad (25)$$

$$Modulation\ factor\ \ m(t) = \alpha \cdot \int_0^t r(t)dt \quad (26)$$

The parameter α was estimated from the simulated result (Fig.3. (d)). The modulation effect is exactly related to the respiratory cycle and volume curve between inspiration and expiration. The curve shows that the induced air flow by HFCC increases during inspiration. Otherwise, it decreases during expiration.

We assumed that each air way generation had one pole and one zero. So we constructed a system model with 23 poles and 23 zeros associated with 23 air way generations including mouth and trachea. Analysis of the 23 generations lung-pleural space-chest wall configuration indicates that the HFCC system is coupled to compliance dominated network.

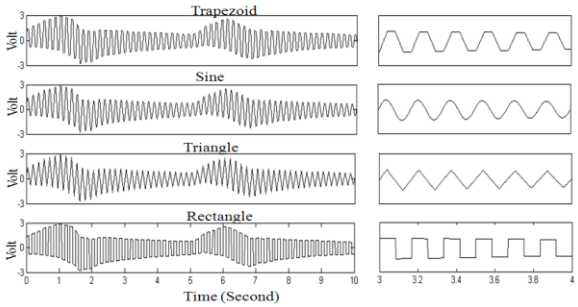

Fig. 5.HFCC simulation of inputs for 10 seconds with two breathing cycles at 6Hz. All inputs were matched at same peak value.

From the standpoint of an airflow-pressure ratio transfer function, resistance-compliance dominated networks were considered for each lung generation. From equation (16), we selected *na* = *nb* =23 and *nk* = 0. In addition, we subtracted each mean value from the input and output data for the offset to construct the system model. Fig.4 shows the poles and zeros of the modeled system as they relate to the unit circle in the z-plane.

For the next step, we simulated two breathing cycles using 4 different inputs: rectangle, sine, triangle and trapezoid waveforms at 6Hz with same peak amplitude (Fig. 5). Then, we observed how each HFCC waveform is changed at the mouth (Fig. 6). We assumed that through the entire

respiratory system is noise free.

Figure 6 shows the results for 10 seconds and 1 second how the HFCC waveforms changes after it travels through the respiratory system. The air flow output signal at the mouth is changed to a triangle waveform from a rectangle waveform input; to sine waveform from triangle waveform; to triangle from trapezoid. However sine waveform does not change as it passes through the respiratory system.

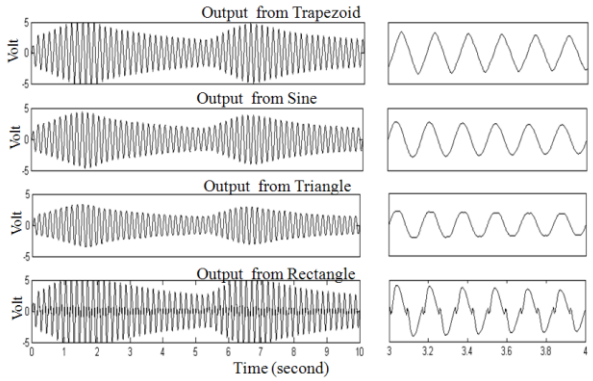

Fig. 6. Simulation of HFCC output signals for the respiratory system. Results show HFCC waveform structure and amplitude changes influenced by the respiratory system.

The maximum inspiratory air flow occurred with rectangle waveform input. The peak inspiratory air flow from trapezoid waveform is about 87% of the rectangle waveform, the peak inspiratory air flow from triangle waveform is about 77% of the rectangle waveform, and the peak inspiratory air flow from sine waveform is about 66% of the rectangle waveform. We also examined that the maximum expiratory air flow occurred from the input of rectangle waveform; trapezoid waveform is about 86% of the rectangle waveform; triangle waveform is about 77% of the rectangle waveform and sine waveform is about 66%.

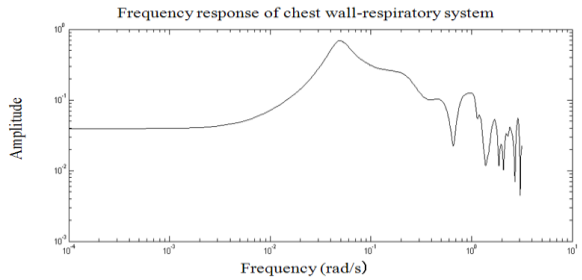

Fig. 7. Frequency response characteristic for the simulated chest wall-lung system.

IV. Conclusion and Discussion

In this study, we investigated the effects of HFCC pulsation to the chest wall-lung system with airflow at the lung and mouth serving as the output parameters of interest. The purpose of this study is to provide additional information on waveform significance. Clinical and laboratory studies using different HFCC show differences in secretion clearance efficacy [18]. Our simulated results show that, as one might expect, the rectangle waveform produced the highest peak air flow. The frequency response of Fig. 7 shows an abrupt cut-off at approximately 0.05 rad/s. This value is a bit low. Other simulations that we have done (unpublished) using lumped R-L-C circuits indicate a cut-off frequency of approximately 4 Hz with a more gradual slope in the frequency response characteristic. The actual cut-off frequency for a large area chest stimulation technique, such as HFCC, is most likely somewhere between 0.5 Hz and 4 Hz. In this study, we assumed that HFCC pressure is uniformly distributed over the chest wall.

References

[1] M. King, D.M. Phillips, D. Wight, D. Gross, H. K. Chang, "Tracheal mucus clearance in high-frequency oscillation effect of peak flow rate bias", *Eur Respir J Suppl,* 1990. **3(1)**: pp. 6-13..

[2] R.P. Tomkiewicz, M. King M, "Effects of oscillation air flow on the rheological properties and clearability of mucous gel stimulants", *Biorheology,* 1994. **31(5)**: p. 511-520..

[3] A. Harf, H.K. Chang, "Nitrogen washout during the tidal breathing with superimposed high-frequency chest wall oscillation", *Am Rev Respir Dis*, 1985. **132**: p. 350-353.

[4] S. Butler, et.al. *"High-frequency chest compression therapy: a case study", Pediatr Pulmonol,* 1995. **19**: p. 56-59.

[5] L. Hansen, and W. J. Warwick. "High frequency chest compression system to aid in clearance of mucus from the lung", *Biomed Instru & Tech,* vol 24,1990,pp289-294

[6] J. Lee, Y. W. Lee and W.J. Warwick. "High Frequency Chest Compression Effects Heart Rate Variability",*.EMBS 2007,29th Annual International Conference of the IEEE 22-26 Aug.2007* page:1066-1069

[7] J. Lee. Y. W. Lee and W.J. Warwick. "High frequency chest compression effects on cardio-respiratory interaction", *Engineering in Medicine and Biology Society, 2008. 30th Annual International Conference of the IEEE* 20-25 Aug. 2008 pages:2447-2450.

[8] A.B. DuBois, A.W. Brody, D. H. Lewis, and B.F. Burgess, "Oscillation mechanics of lungs and chest in man," *Journal of Applied Physiology*, Vol. 8, pp, 587-594, 1956

[9] M.Schmidt, B. Foitzik, O. Hochmuth, and G. Schmalisch, "Computer simulation of the measured respiratory impedance in newborn infants and the effect of the measurement equipment,"*Medical Engineering & Physic*, vol. 20,pp.220-228,1998

[10] T.Woo, B. Diong, L. Mansfield, M. Goldman, P. Nava and H. Nazeran, "A comparison of various respiratory system models based on parameter estimates from Impulse Oscillometry data", *Proc. IEEE Engineering Medicine Biology Conf., San Francisco, CA, Sep 2004*

[11] K.R. Lutchen, "Optimal selection of frequencies for estimating parameters from respiratory impedance data," *IEEE Transactions on Biomedical Engineering*, vol.35, no. 8, pp. 607-617,1988

[12] K.R. Lutchen and K.D. Costa, " Physiological interpretations based on lumped element models fit to respiratory impedance data: use of forward-inverse modeling," *IEEE Transactions on Biomedical Engineering* , vol. 37, no. 11, pp.1076-1086,1990

[13] K. Sohn, J.E. Holte, J.R. Phillips, W.J. Warwick, "Modeled velocity of airflow in the airways during various respiratory patterns,"*26thAnnaul International Conference of the IEEE EMBS,* 2004, pp3925-3928.

[14] Y. W. Lee, J. Lee, and W.J. Warwick, "Two Models of High Frequency Chest Compression Therapy: Interaction of Jacket Pressure and mouth Airflow," *26thAnnaul International Conference of the IEEE EMBS,2007*,pp 4243-4246

[15] L. Ljung, *SYSTEM IDENTIFICATION: Theory for the User* (Book style). Englewood Cliffs, NJ: Prentice Hall, 1998

[16] U. Forssell and L. Ljung, "Closed-loop identification revisited," *Automatica*,vol. 35, pp. 1215–1241, 1999.

[17] Y. Zhao and R. E. Kearney, "Closed-Loop System Identification of Ankle Dynamics with Compliant Loads", *Proceedings of EMBS,2007*, Lyon, France

[18] C.E. Milla, L.G. Hansen, A. Weber, W.J. Warwick, "High-Frequency Chest Compression, Effect of the Third Generation Compression Waveform", *Biomedical instrumentation & Technology,* 2004 (JUL.-AUG.). **38**(Issue 4): p. 322-328.